

# Supporting Information

Wei et al. 10.1073/pnas.1217931110

## SI Text

**Near-Field Distribution for Different Incident Polarization.** When the laser is polarized along the nanowire (NW), only  $H_0$  and  $H_2$  modes are excited, and plasmon beating along the NW shows the quasiperiodic pattern (Fig. S2*Ai*). As the polarization is rotated away from the parallel direction, besides  $H_0$  and  $H_2$  modes,  $H_1$  mode is excited, which shifts the near-field intensity pattern as can be seen from Fig. S2*Aii* and *Aiv*. If the laser is polarized perpendicular to the NW,  $H_1$  mode is mainly excited and the near-field intensity is aligned at the sides of the NW (Fig. S2*Aiii*). For the NW in Fig. S2*B*, as the laser polarization is close to the perpendicular direction, the near-field pattern becomes more complex. When the laser is polarized perpendicular to the NW, the near-field intensity is distributed on the two sides of the NW (Fig. S2*Biv*). The higher-order modes can also be excited because this wire is thicker. The shorter-period near-field modulation

pattern in Fig. S2*Biv* could be caused by the interference of  $H_1$  mode and the higher-order mode.

**Propagation Constants for NWs of Different Radius.** With the increase of the coating thickness, the  $\text{Re}(\Delta k_{//})$  decreases and approaches a minimum as shown in Fig. S5*A*. However, because the refractive index of the coating layer, i.e.,  $\text{Al}_2\text{O}_3$ , is larger than that of the substrate, further increasing the coating thickness ( $T > 94$  nm) introduces new asymmetry in the dielectric environment.  $\text{Re}(\Delta k_{//})$  increases a bit and eventually saturates to a value corresponding to the case of a NW at the glass- $\text{Al}_2\text{O}_3$  interface. If the refractive index of the coating layer is the same as the substrate, the  $\text{Re}(\Delta k_{//})$  decreases monotonically with the increase of the coating thickness and becomes saturated for very thick coating (Fig. S5*B*).

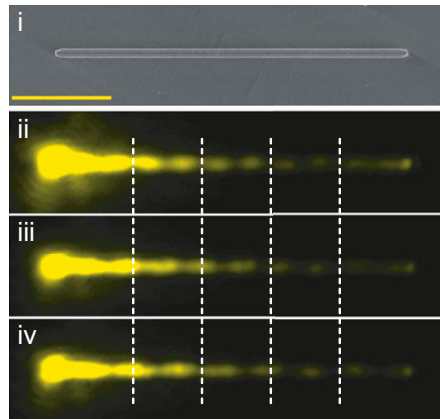


**Fig. S1.** Near-field distribution changes when additional  $\text{Al}_2\text{O}_3$  is deposited on top of the quantum dots. (i) The SEM image for a NW of 167-nm radius with  $\text{Al}_2\text{O}_3$  coating of 30-nm thickness. (Scale bar, 5  $\mu\text{m}$ .) (ii–iv) The near-field distribution measured in air (ii), and then after depositing 5 nm of  $\text{Al}_2\text{O}_3$  (iii), and finally with an additional 5 nm of  $\text{Al}_2\text{O}_3$  (iv). The white dashed lines are visual guides to show the shift of the plasmon near-field pattern.

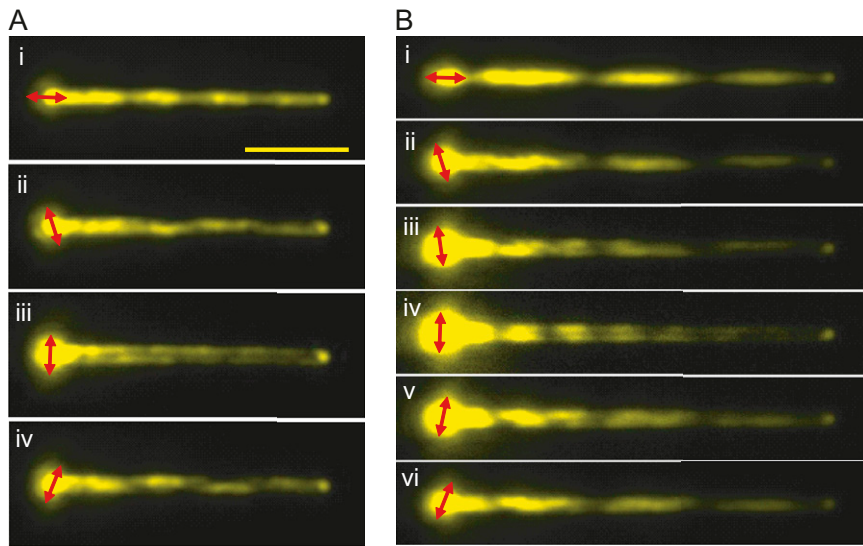


**Fig. 52.** The near-field distribution for different incident polarization for NWs coated by  $\text{Al}_2\text{O}_3$  layer of thickness  $T = 50$  nm (A) and  $T = 80$  nm (B). The radiuses of the NWs in A and B are 150 and 180 nm, respectively. (Scale bar in A for A and B, 5  $\mu\text{m}$ .)

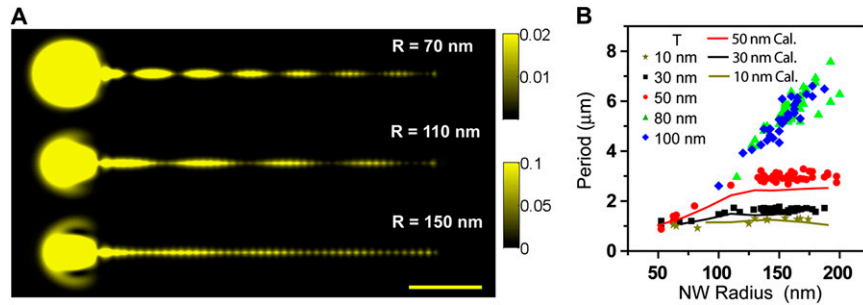


**Fig. 53.** (A) Three-dimensional finite difference time domain (FDTD) calculated electric field intensity distribution in the  $xy$  plane for NWs of difference radius. The coating thickness  $T$  is 50 nm. (Scale bar, 2  $\mu\text{m}$ .) (B) Comparison of FDTD calculated (lines) beat period and measured data (dots) for thin coatings. The measured data are the same as in Fig. 3A. The calculated beat periods are obtained from the near-field distribution. The incident excitation is the same as in Fig. 2.

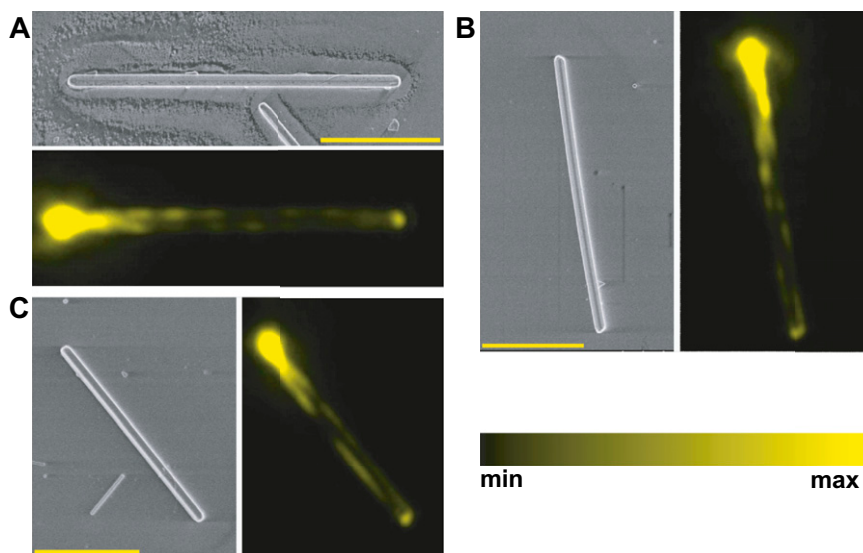


**Fig. 54.** SEM (Upper/Left) and near-field distribution (Lower/Right) images for thick NWs. The radiuses of the NWs are 217 nm in A, 222 nm in B, and 232 nm in C. The  $\text{Al}_2\text{O}_3$  thickness is 30 nm. (Scale bars, 5  $\mu\text{m}$ .)

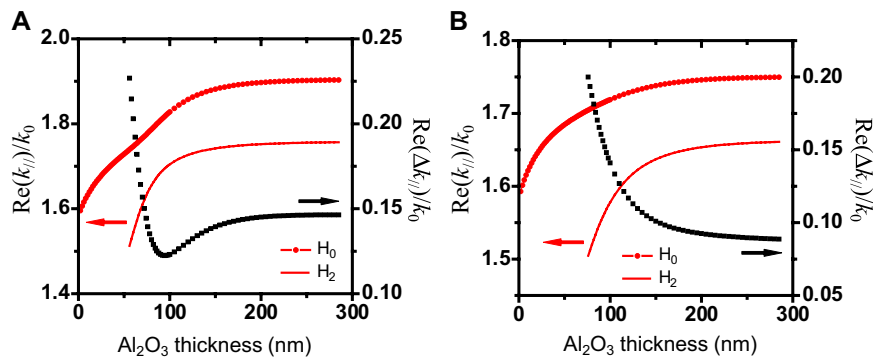


**Fig. S5.** (A) Extended plot of Fig. 3D, showing the real part of the propagation constant of the  $H_0$  and  $H_2$  mode for larger  $\text{Al}_2\text{O}_3$  coating thickness. The difference of the propagation constants is also included. (B) The same as A except the refractive index of the coating layer is set to 1.5, equal to that of the substrate.

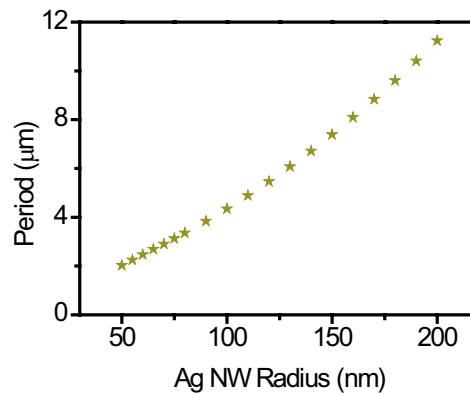


**Fig. S6.** FDTD calculated beat period for NWs in a uniform medium of air as a function of Ag NW radius. The NWs are coated by  $\text{Al}_2\text{O}_3$  layer of 10-nm thickness. Cylindrical cross-sections are used in these calculations.

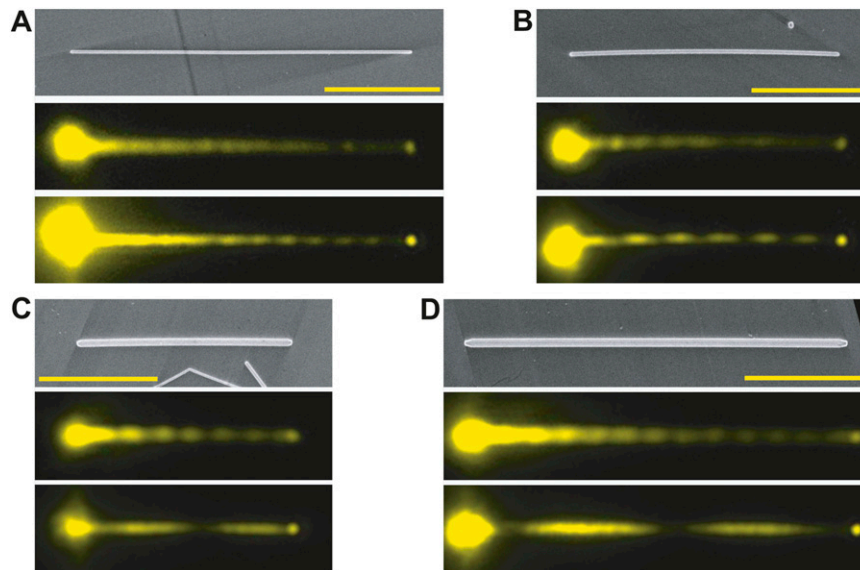


**Fig. S7.** Near-field distribution for NWs of different radius. The  $\text{Al}_2\text{O}_3$  coating thickness is 10 nm. The quantum dot emission images are measured in air (Middle) and oil (Bottom). The radii of the NWs in A–D are 51, 72, 134, and 162 nm, respectively. (Scale bars, 5  $\mu\text{m}$ .) The top panels are SEM images of the NWs. By comparing the bottom panels from A to D, it can be seen that the beat period increases monotonically with NW radius when the NWs are in a homogenous environment.